Available online at www.sciencedirect.com

SCIENCE DIRECT®

Journal of Nuclear Materials 337–339 (2005) 441–445

journal of nuclear materials

www.elsevier.com/locate/jnucmat

Fuelling efficiency of hydrocarbons in TJ-II plasmas

I. García-Cortés *, F.L. Tabarés, D. Tafalla, A. Hidalgo, J.M. Carmona, K.J. McCarthy, F. Medina

Laboratorio Nacional de Fusión. Asociación Euratom/Ciemat, Avda. Complutense 22, 28040 Madrid, Spain

Abstract

Carbon fuelling experiments have been performed in ECRH TJ-II plasmas by injecting C_2H_4 (ethylene) at several radial positions through gas injection ports located on poloidal diagnosted limiters. Simultaneous plasma edge characterization has been performed with atomic beams (He, Li) and by emission spectroscopy. From comparisons of plasmas having He and H as the main species it has been determined that physical sputtering in the interaction region between the plasma and the vacuum vessel is the source of intrinsic carbon contamination. Target plasmas with a range of magnetic configurations and having different edge topologies have been also used. In particular, configurations with rational numbers that result in island chains at the edge have been explored for possible application as 'divertor-type' plasmas. Fuelling efficiencies of a few percent for injected carbon have been deduced and clear enhanced screening for chemically bounded carbon is observed to occur in the presence of peripheral magnetic islands.

PACS: 52.55.Hc
Keywords: TJ-II; ECRH; Island divertor; Carbon impurities; Impurity transport

1. Introduction

Hydrocarbon transport is a highly relevant issue for carbon-based divertor machines as it is closely related to erosion, re-deposition and tritium trapping phenomena [1]. Although extensive work in this field has been carried out for tokamaks [2], to date scant information exists for stellarator machines. Their unique edge topology, with a direct impact on peripheral impurity transport, makes such studies crucial both for enhancing the current understanding of carbon migration in fusion devices as well as for predicting its behaviour in future stellarator-based reactors [3]. For instance, the high efficiency of divertor configurations in W-7AS has permitted the high-density H-mode to be achieved, with record values of plasma density and energy content, even for the relatively small associated plasma volume [4]. In TJ-II, the use of edge island-configurations could help in contaminant control and thus total radiation during the NBI phase required for high beta operation.

From the atomic physics point of view, hydrocarbon transport is still a challenging topic that involves the interplay of a large number of idly characterized basic processes. Validation of current carbon transport codes [5] is an urgent task with implications for the choice of reactor first-wall materials. Well-characterized plasma edge conditions and extensive diagnostics of the physico-chemical mechanisms of carbon transport are a basic

* Corresponding author. Tel.: +34 913 466 515; fax: +34 913 466 124.
E-mail addresses: Isabel.GarciaCortes@ciemat.es (I. García-Cortés), david.tafalla@ciemat.es (D. Tafalla).

0022-3115/$ - see front matter
doi:10.1016/j.jnucmat.2004.07.055

pre-requisite for this goal. In many respects, the excellent transport frame provided by externally generated magnetic configurations in stellarators can be of great help in experiment planning and interpretation. In this work, a first characterization of the peculiarities of hydrocarbon transport in stellarator plasmas has been carried out. For this, ethylene was chosen because of its expected relevance in high-density divertor plasmas [6].

In this paper, the set-up is described in Part 2. The results concerning the main source of carbon contamination in ECRH TJ-II plasmas are described in Part 3. In addition, the behaviour of externally injected carbon, in terms of its contribution to the total plasma content is addressed. The effect of edge topology in the contamination efficiency of intrinsic and injected carbon sources is also analysed in Part 3. Finally, in Part 4 the results are interpreted under the light of previous findings and of the peculiarities of stellarator plasmas.

2. Experimental

TJ-II is a medium-sized stellarator with a large magnetic flexibility. It is a four-period, low magnetic shear, device ($R = 1.5$ m, $B_T = 1$ T, $t_{pulse} \leqslant 300$ ms, $0.9 \leqslant \iota(0)/2\pi \leqslant 2.2$) [7]. The plasma cross-section is bean shaped, $\langle a \rangle = 0.22$ m. Plasma heating is produced by ECRH ($P \leqslant 400$ kW, $n_e(0) \leqslant 1.7 \times 10^{19}$ m^{-3} and $T_e(0) \leqslant 2$ keV) and NBI ($P < 500$ kW predicted) with hydrogen as the main plasma species. TJ-II is a limiter machine with its last closed flux surface (LCFS) defined by either its two movable graphite poloidal limiters or by its helical one (i.e. the inner side of the vacuum chamber). In the experiments reported here, the inner wall was boronised and very low Z_{eff} values were inferred from radiation diagnostics [8].

The target plasmas used in these experiments have been created using a variety of magnetic configurations. In particular, configurations having rational numbers that result in island chains at the edge were explored for possible application in 'divertor-type' plasmas, one example being plotted in Fig. 1(a). In particular, impurity/carbon screening was systematically studied and compared for plasmas confined in a 'standard' magnetic configuration (see Fig. 1(b)) and in 'divertor-type' configurations.

The carbon transport/fuelling experiments were performed in TJ-II by injecting C_2H_4 (ethylene) through an aperture in two mobile poloidal limiters that allow the plasma minor radius to be varied from the vessel wall position to a position (2–3 cm) inside the LCFS, depending on the magnetic configuration. Gas was normally injected at a constant flow rate for a fixed period of typically 15 ms during the steady state period of the discharge thereby allowing comparisons to be made of

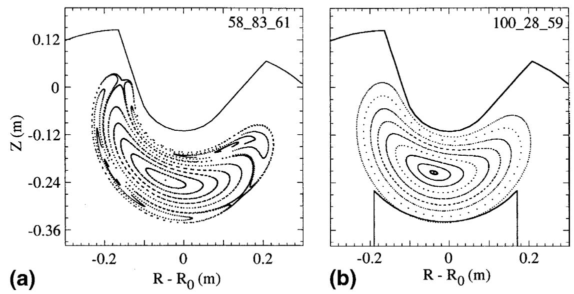

Fig. 1. Two examples of the magnetic configurations used in the experiments. LHS: an example of a 'divertor-type' configuration and RHS: a 'standard' configuration.

impurity transport before and after the puff injection as well as between discharges.

Finally, numerous diagnostics were employed to monitor specific and general plasma behaviour during these experiments. For instance, characterization of the plasma edge was performed with atomic beams (He, Li) to provide density and temperature profiles [9], as well as with VUV and visible emission spectroscopy [10]. Simultaneously, five 16-channel soft X-ray arrays were used to tomographically reconstruct the emissivity profile and also to estimate the increments of Z_{eff} due to the puffing of ethylene [11].

3. Results

Under typical ECRH plasma operation with boronised walls, carbon appears as the main plasma contaminant in TJ-II. Although two poloidal graphite limiters are used to define the LCFS, their insertion into the plasma edge did not give rise to enhanced carbon contamination for displacements of $\leqslant$2–3 cm inwards from the nominal LCFS position. This points to the vacuum vessel as being the main impurity source. Indeed, particularly strong interaction is expected from that part of the vessel covering the central coils (H.C.). In order to characterize the intrinsic carbon generation mechanism, the evolution of central (C V and C VI) and peripheral (C III) carbon signals were recorded in both hydrogen and helium plasmas. Edge densities $n_e(a) \sim (1–2) \times 10^{12}$ cm^{-3} and electron temperatures $T_e(a) \sim (30–40)$ eV were measured for both plasma types [9]. In Fig. 2, the normalized C V intensity (integrated over the whole plasma volume) is plotted as a function of line density. Data for two magnetic configurations (an example of each is in Fig. 1) corresponding to 'standard' and 'divertor-type' cases are displayed. As can be observed, a factor of two lower normalized values of C V were recorded for 'divertor-type' configurations. Similar behaviour was detected for the C VI emissions and for normalized bolometer signals, thus confirming the

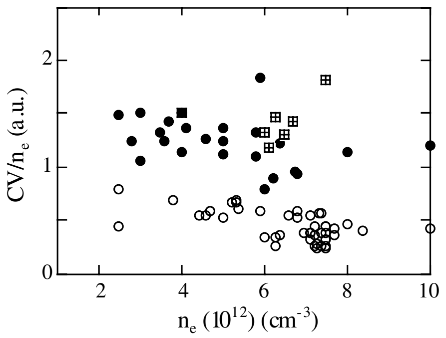

Fig. 2. Normalized C V emission versus line averaged density. Open circles are plasmas in 'divertor-type' configurations and the rest are for 'standard' configurations, the closed circles are for H as the main plasma species and the squares-crosses for He.

relevance of carbon for the total impurity content, while soft X-rays profiles became narrower for the 'divertor-type' case. Also, the decrease in confined impurity content evident for 'divertor-type' configurations for intrinsic generation cannot be directly ascribed to either of the two obvious mechanisms involved, i.e. generation and screening of carbon species. Also, it should be noted that little or no evolution of carbon content with line density is recorded in the cases in Fig. 2. This fact is well correlated with the relative insensitivity of edge parameters to line density in TJ-II ECRH plasmas. Similarly, H and He plasmas are compared for a 'standard' configuration in Fig. 2 (squares with crosses). As seen, no significant differences with regard to carbon concentration appear when H is replaced by He as the working gas, thus precluding chemical sputtering as the main carbon contributor in TJ-II ECRH plasmas.

The effect of plasma edge on carbon screening has been studied by injecting ethylene, through the movable limiters, into hydrogen plasmas. A steady flow of ethylene, as recorded by expansion into the vessel between discharges was used, although some variations were found by simultaneous measurements of the H_α and CH emissions arising from the cracking of ethylene at the edge. Thus, normalized quantities of the hydrocarbon flow to these emissions are used for comparative studies. In Fig. 3, the time evolution of some characteristic traces during hydrocarbon injection is displayed. A ~40 ms delay due to the restricted conductance of the pipe coupled to the limiter was determined. Thus, although the nominal setting for open the valve was 1130–1145 ms, no effect was observed before 1170 ms. As shown, a significant increase in carbon-related and radiation signals takes place upon injection, insignificant changes occur in traces related to global plasma parameters. Also, measurements by the atomic beam diagnostic indicated that no significant cooling of the edge occurred.

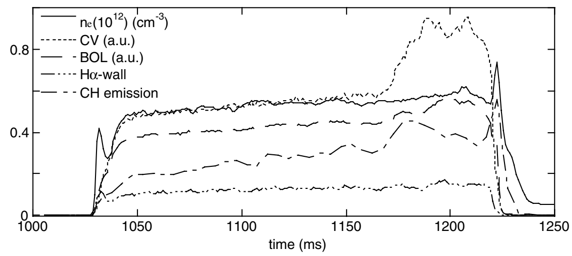

Fig. 3. Time evolution of plasma general traces. See text for explanation.

The sensitivity of plasma contamination to impurity source location was also studied by inserting one of the gas-puff limiters (while maintaining other parameters such as the position of the other limiter constant). Again, the increment of the normalized C V signal was used as a reference for the confined carbon concentration. The experiments were performed for 'divertor-type' and 'standard' configurations, and the range of limiter displacements is displayed in Fig. 1 for these cases. The data were normalized for shot-to-shot variations of injected flow, as described previously. As shown in Fig. 4, for the 'standard' configuration a systematic increase of central carbon is observed as ethylene is puffed further into the plasma, i.e. beyond the LCFS nominal position. An increase of a factor of 3 between the two extreme positions, i.e. ~20 mm apart, was recorded. In contrast, no measurable increase was observed for the same spatial range in the configuration with edge islands. However, a dramatic increase of the contamination efficiency for the injected hydrocarbon occurs when the gas source reaches the first closed magnetic surface defining the main plasma. Interestingly, extrapolation of the data for the 'standard' configuration would yield a very similar value, thereby suggesting that the

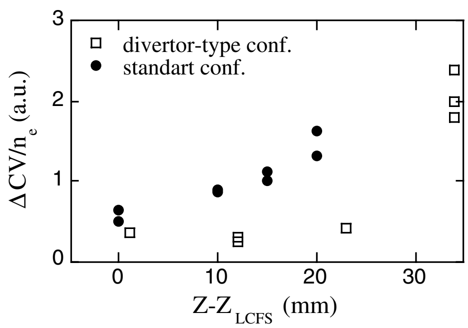

Fig. 4. Evaluation of the normalized C V contamination at different radial position of the impurity puff, for both configurations: Closed circles for 'standard' and open squares for 'divertor-type' configurations.

effect is associated with the edge configuration rather than with the main confinement properties.

Finally, it is worth noting that as a systematic feature, puffing of ethylene to inner positions led to the production of spikes in C V and radiation detectors. These spikes were not recorded in H_α or CH signals coming from the limiter, and they disappeared after a few repetitive shots. A likely source could be a loosely bounded carbon film produced during local hydrocarbon puffing [12], and their production would therefore be an indication of efficient carbon re-deposition under the experimental conditions here explored.

4. Discussion

For externally injected impurities, the absolute fuelling efficiency can be estimated from the input flow, Q_c, by using the expression [13]:

$$\mathrm{FE} = N_c/Q_c \cdot \tau_I, \quad (1)$$

where N_c is confined carbon density and τ_I is impurity confinement time. Significant screening can be expected when an impurity is injected at the scrape-off-layer (SOL), in particular for non-recycling impurities such as carbon. In order to quantify such screening, one can use the predictions of simple models relating injected impurity flow to central impurity concentration [14], e.g. the Engelhart model,

$$N_c = Q_c \cdot \lambda_{SOL} \cdot V_{pl}/D \cdot S_{pl} \cdot \exp -(r_{iz} - r_{SOL})/\lambda_{SOL}, \quad (2)$$

where S_{pl} and V_{pl} are plasma volume and total surface ($0.6\,m^3$, $10\,m^2$ respectively) and λ_{SOL} is density decay length at the SOL, and transport is characterized by a diffusion coefficient, D. Although this model was initially developed for tokamaks with ergodic divertors, its use in stellarators as the Wendelstein 7-AS, where some of the intrinsic assumptions of the model are not fully justified, has already provided reasonable estimates of impurity screening [15]. As seen in Eq. (2), an exponential increase in central impurity concentration is predicted by the model as the ionisation location gets closer to the LCFS. Combining Eqs. (1) and (2) provides an expression for the fuelling efficiency, FE, which is independent of the gas flow value, i.e.

$$\mathrm{FE} = V_{pl} \cdot \lambda_{SOL}/D \cdot S_{pl} \cdot \tau_I . \exp -(r_{iz} - r_{SOL})/\lambda_{SOL.} \quad (3)$$

Measurements of the TJ-II SOL region [16] have provided figures for these parameters. Typical values are 1 cm and $10^4\,cm^2\,s^{-1}$ for the SOL decay length and diffusion coefficient respectively. Inserting these into Eq. (3), and assuming the same confinement time for particles and impurities (~10 ms), allows one to estimate the expected fuelling efficiency for injected ethylene. For the plasma parameters at the SOL, the ionisation mean free path of this species is <1 cm. Although the limiter insertion experiments were initiated at the nominal location of the LCFS, the predicted carbon concentration for $r_{iz} = r_{SOL}$ is much higher than that inferred from radiation diagnostics, even for the outermost position. However, values of increased carbon concentration between 0.8% and 2% can be inferred from the equation if one assumes that the actual location of the LCFS (i.e. the confinement boundary) is located 2–3 cm inwards from the nominal one. This would be also consistent with the lack of contamination by the poloidal limiters as they are inserted into the plasma by an equivalent length. The reason for the existence of this intermediate, weakly confining, region is not clear, but it might be related to the strong magnetic ripple of the TJ-II plasma periphery.

For physically sputtered carbon, which has a much higher penetration depth, the situation is expected to be different. In a steady state model of carbon impurity generation by the combined effects of physical sputtering by plasma particles and light impurities (including self-sputtering) we have

$$dN_c/dt = (\Gamma_H \cdot \gamma_H + \Gamma_C \cdot \gamma_C)/V_{pl} - N_c/\tau_I = 0, \quad (4)$$

where the usual symbols for fluxes and sputtering yields have been used. For simplicity, carbon is considered as the only light impurity here. Then, assuming that the ratio of C/H flows equals that of their corresponding content in the plasma (equal confinement) an expression can be deduced for carbon contamination having the form

$$N_c/n_e = (\Gamma_H \cdot \gamma_H) \cdot \tau_I/(V_{pl} \cdot n_e - \tau_I \cdot \Gamma_H \cdot \gamma_C). \quad (5)$$

As seen, the ratio of the sputtering yields for carbon by H and by itself basically determines the degree of plasma contamination if full ionisation of the resulting atoms is assumed. For Z_{eff} values of ~1.5, the concentration of fully ionised carbon is ~1%. This implies $\gamma_H + \gamma_C/100 = 0.01$, which is in good agreement with expected values for energies between 100–150 eV and with measured edge temperatures.

However, in order to explain the systematic lower values of intrinsic carbon signals in edge-island configurations, the extra contribution of the lower edge temperatures to the impurity production has to be properly considered. In this respect, the lower C III signal values detected in such cases are a good indication of reduced interaction with the vessel walls as schematically displayed in Fig. 1. Further work, devoted to the separate characterization of the generation and confinement of impurities under these special configurations, is currently being undertaken.

5. Conclusions

The fuelling efficiency of intrinsic and injected carbon impurities has been investigated in TJ-II plasmas for several magnetic configurations and several finding were made. For instance, it was found that physical sputtering at the main vessel seems to be the source of intrinsic contamination under normal, limiter operation. Furthermore, efficient screening of molecular impurities was found by performing ethylene injection experiments. The application of a simple screening model suggests the existence of a weak confinement or enhanced transport region inwards from the LCFS for normal configurations. In addition, enhanced screening of injected impurities was found to occur in edge island configurations, thereby leading to very clean ECRH plasmas. A lower interaction with the wall also led to lower intrinsic impurity content.

Acknowledgments

This work has been partially supported by the Dirección General de Investigación Científica y Técnica (DGICYT) under Project FTN2000-0915-C03-01. The authors would also like to thank Alberto Loarte for his help and for useful discussion.

References

[1] G. Federici et al., J. Nucl. Mater. 290–293 (2001) 260.
[2] G. McCracken et al., Nucl. Fusion 33 (1993) 1409.
[3] J. Nührenberg et al., Trans. Fusion Technol. 27 (1995) 71.
[4] K. McCormic et al., J. Nucl. Mater. 313–316 (2003) 1131.
[5] J.N. Brooks, D.N. Ruzic, J. Nucl. Mater. 176&177 (1990) 278.
[6] J. Roth et al., Atomic and Plasma-Material Interaction Data for Fusion (Suppl. to Nucl. Fusion), vol. 1, IAEA, Vienna, 1991, p. 63.
[7] C. Alejaldre et al., Plasma Phys. Control Fusion 41 (1999) A539.
[8] F. Tabarés et al., J. Nucl. Mater. 313–316 (2003) 839.
[9] B. Brañas et al., Rev. Sci. Instrum. 72 (2001) 602.
[10] K.J. McCarthy et al., Fusion Sci. Technol. 46 (2004) 129.
[11] F. Medina et al., Rev. Sci. Instrum. 70 (1999) 642.
[12] M. Stamp, these Proceedings, doi:10.1016/j.jnucmat.2004.07.061.
[13] J. Strachan et al., Nucl. Fusion 43 (2003) 922.
[14] P.C. Stangeby, G.M. McCracken, Nucl. Fusion 30 (1990) 1225.
[15] D. Hildebrandt et al., J. Nucl. Mater. 220–222 (1995) 703.
[16] F. Tabarés et al., J. Nucl. Mater. 290 (2001) 748.